Supplemental material for "*Using a deep neural network to detect methane point sources and quantify emissions from PRISMA hyperspectral satellite images*"

Peter Joyce[1,2,3], Cristina Ruiz Villena[4,5], Yahui Huang[2,3], Alex Webb[4,5], Manuel Gloor[1], Fabien H. Wagner[6,7], Martyn P. Chipperfield[2,3], Rocío Barrio Guilló[4], Chris Wilson[2,3], and Hartmut Boesch[4,5]

[1]*School of Geography, University of Leeds, Leeds, United Kingdom*

[2]*National Centre for Earth Observation, University of Leeds, Leeds, United Kingdom*

[3]*School of Earth and Environment, University of Leeds, Leeds, United Kingdom*

[4]*University of Leicester, Leicester, United Kingdom*

[5]*National Centre for Earth Observation, University of Leicester, Leicester, United Kingdom*

[6]*Institute of Environment and Sustainability, University of California, Los Angeles, CA, USA*

[7]*Jet Propulsion Laboratory, California Institute of Technology, 4800 Oak Grove, Pasadena, CA 91109, USA*

This file contains the following:

Figure S1- Wind speed of the training and validation images used in this paper. Colour scale indicates number of images with each wind speed.

Figure S2- Mix depth of the training and validation images used in this paper. Colour scale indicates number of images with each mix depth.

Figure S3- Plume time step (s) of the training and validation images used in this paper. Colour scale indicates number of images with each time step.

Figure S4- Emission rate of the training and validation images used in this paper. Colour scale indicates number of images with each emission rate.

Table S1- Locations of PRISMA scenes used to make training, validation, and testing data.

Table S2- Mean and standard deviation of the noise and methane concentrations of the false positives and false negatives described in Table 1.

Table S3- Plumes found in the Korpeje oil field using the neural network.

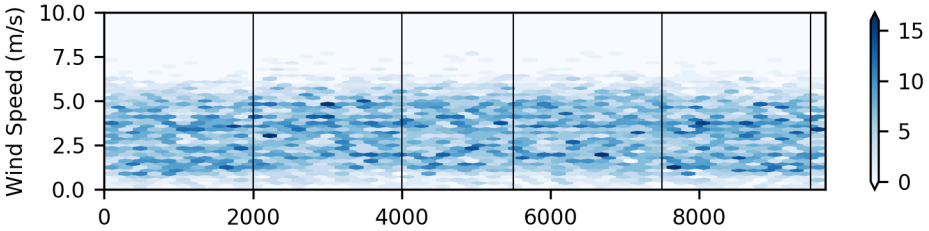

Figure S1: Wind speed of the training and validation images used in this paper. Colour scale indicates number of images with each wind speed.

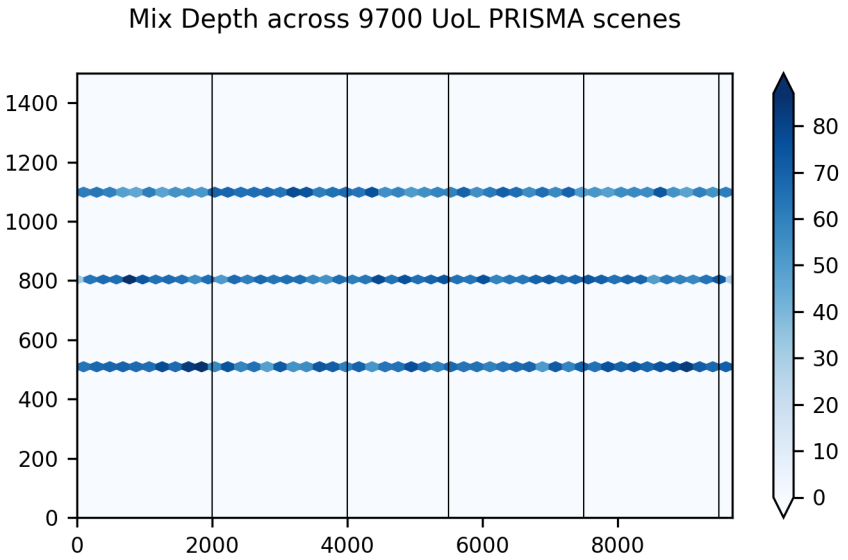

Figure S2: Mix depth of the training and validation images used in this paper. Colour scale indicates number of images with each mix depth.

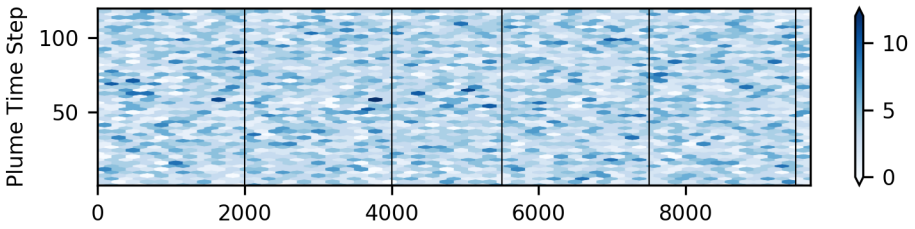

Figure S3: Plume time step (s) of the training and validation images used in this paper. Colour scale indicates number of images with each time step.

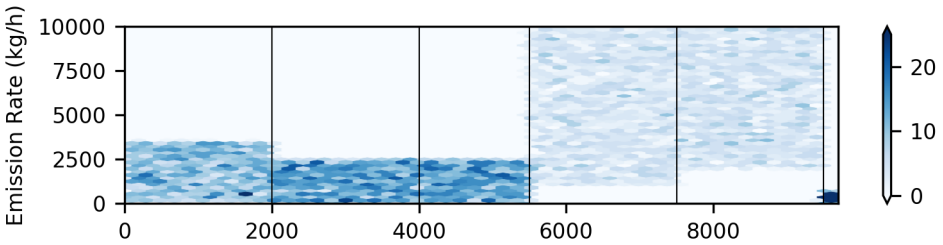

Figure S4: Emission rate of the training and validation images used in this paper. Colour scale indicates number of images with each emission rate.

Table S1: Locations of PRISMA scenes used to make training, validation, and testing data. Right column lists of numbers detail the number of different training images made using the corresponding scene in the left column. Each value in the list corresponds to a different PRISMA scene.

Scene location	Number of images made
Brazil	412, 437
Canada	442, 437
Iraq	151, 161, 159, 154, 149, 16
Iran	169, 14, 15, 12, 21, 15, 18, 15
Saudi Arabia	18, 16, 21, 12, 7
South Africa	434, 407, 418, 421, 449, 438
Texas	147, 157, 143, 183, 170, 428, 417
Turkmenistan	152, 167, 145, 168, 153, 162, 140, 155, 147, 431, 390, 450

Table S2. Mean and standard deviation of the noise and methane concentrations of the false positives and false negatives described in Table 1.

	Mean, std of scene noise (PSNR)	Mean, std of max methane concentration (1e18 molecules cm^{-2})
True positive	20,5	49,
True negative	18,5	N/A
False positive	20, 5	N/A
False negative	17, 5	10, 9

Table S3. Plumes found in the Korpeje oil field using the neural network. PRISMA scene code indicated on the far left, with 'PRS_L1_STD_OFFL_' from the beginning for brevity. Coordinates of the centre of the plume and estimated emission rate are detailed in the right-most columns.

Scene code	Plume number	Coords of plume (x,y)	Emission rate (kg/hr)
20210209072220_20210209072224_0001	1	314, 420	1112
20210310072149_20210310072153_0001	2	323, 405	1281
20210414072435_20210414072439_0001	3	307, 422	1134
20210622071436_20210622071440_0001	4	420, 300	6249
20210721071449_20210721071453_0001	5	309, 427	3008
20210808072451_20210808072455_0001	6	537, 456	2726
20200419072133_20200419072138_0001	7	916, 84	2098
	8	301, 409	2906
20200703071439_20200703071443_0001	9	299, 381	4841
	10	548, 410	1539
	11	548, 456	1885
20200721072426_20200721072430_0001	12	320, 411	7615
	13	489, 432	2370
20200807071742_20200807071747_0001	14	335, 450	5204
20201010072033_20201010072038_0001	15	329, 407	1769
20201114072336_20201114072341_0001	16	469, 362	2332
20220327071152_20220327071156_0001	17	431, 351	3038
	18	480, 569	3591
	19	480, 584	5263
20220524071139_20220524071144_0001	20	411, 282	2465
20211219071850_20211219071854_0001	21	268, 704	5304